

# Evanescent Bloch waves and the complex band structure of phononic crystals

Vincent Laude, Younes Achaoui, Sarah Benchabane, and Abdelkrim Khelif

*Institut FEMTO-ST, Université de Franche-Comté, CNRS, ENSMM, UTBM, 32 Avenue de l'Observatoire, F-25044 Besançon Cedex, France*

(Received 6 March 2009; revised manuscript received 16 June 2009; published 18 September 2009)

The complex band structure of a phononic crystal is composed of both propagating and evanescent Bloch waves. Evanescent Bloch waves are involved in the diffraction of acoustic phonons at the interfaces of finite phononic crystal structures. They are shown to arise both because of band gaps, where they directly measure the exponential decrease upon transmission, and because of the frustrated nature of higher-order diffracted waves at low frequencies. These diffracted evanescent Bloch waves become propagative as the frequency increases thus populating higher frequency bands. These results should apply as well to any periodic medium supporting the propagation of waves.

DOI: [10.1103/PhysRevB.80.092301](https://doi.org/10.1103/PhysRevB.80.092301)

PACS number(s): 43.20.+g, 43.35.+d, 77.65.Dg

Evanescent waves are particular solutions of the wave equation that decay or increase exponentially with distance. They are involved in many physical phenomena including coupling in and out waveguides and resonators,<sup>1</sup> near-field optics,<sup>2</sup> tunneling,<sup>3,4</sup> subwavelength focusing,<sup>5-7</sup> or surface waves.<sup>8,9</sup> A well known and simple example is provided by the one-dimensional diffraction grating depicted in Fig. 1(a). An incident plane wave with angular frequency  $\omega$  and wave vector  $\mathbf{k}$  has an amplitude proportional to  $\exp[-i(k_1x_1 + k_2x_2)]$ . The field diffracted by the grating is composed of a superposition of plane waves

$$u(x_1, x_2) = \sum_n a_n \exp[-i(k_{1n}x_1 + k_{2n}x_2)], \quad (1)$$

$$k_{2n} = k_2 + n \frac{2\pi}{a}, \quad k_{1n} = \sqrt{\frac{\omega^2}{v^2} - k_{2n}^2}, \quad (2)$$

where  $v$  is the velocity for the particular kind of wave considered. In Eq. (1), every Fourier harmonic has amplitude  $a_n$  and the wave vector component  $k_{1n}$  is either a real or a purely imaginary complex number, depending on the sign of the expression under the square root in Eq. (2). At a given frequency  $\omega$ , evanescent waves are characterized by the fact that their wave vector,  $\mathbf{k}(\omega)$ , is complex valued. In the simple grating model above, each diffracted wave with  $n \neq 0$  becomes evanescent under the cut-off frequency  $\omega_n = k_{2n}v$  but is propagative above it.

Of special interest is wave propagation in periodic media, including photonic<sup>10,11</sup> and phononic crystals.<sup>12</sup> In these artificial crystals, the contrast of material constants is purposely made very high between different materials that are repeated periodically along two or three directions of space. Band structures are used to summarize the dispersion relations of propagating Bloch waves. One of the most important features of photonic and phononic crystals, however, is the possible existence of complete band gaps, or frequency ranges inside which any propagating Bloch waves is forbidden, whatever the direction of incidence and the polarization. Complete band gaps are for instance required for defect-based energy trapping, filtering, or wave guiding.<sup>13,14</sup> Since propagation is inhibited within a frequency band gap, only

evanescent waves are left to explain the exponentially decreasing transmission of waves, and traditional band structures are of no help. Engelen *et al.*<sup>9</sup> have recently measured the decay of the evanescent field of a composite Bloch wave in the near field of a photonic crystal waveguide and found this decay to be multiexponential. In this paper, we discuss the evanescent Bloch wave solutions of phononic crystals and the associated complex band structures. Though it has been remarked that nothing in the Bloch theorem prevents the Bloch wave vector from assuming complex values,<sup>15</sup> the physical status of the latter is uncertain. The layer multiple-scattering method, for instance, naturally allows one to retrieve complex solutions and has been used with success within frequency band gaps.<sup>16</sup> For photonic crystals, Hsue *et al.* have proposed an extended plane-wave expansion (PWE) method and have discussed some of the properties of the complex solutions,<sup>15</sup> especially in relation with the completeness of the basis they provide for scattering problems. Similarly, evanescent Bloch waves are involved in the diffraction of acoustic phonons at the interfaces of finite phononic crystal structures. The extended phononic PWE method derived in this paper allows us to obtain full complex band structures and to relate evanescent Bloch waves to diffracted waves in the phononic crystal for all frequencies.

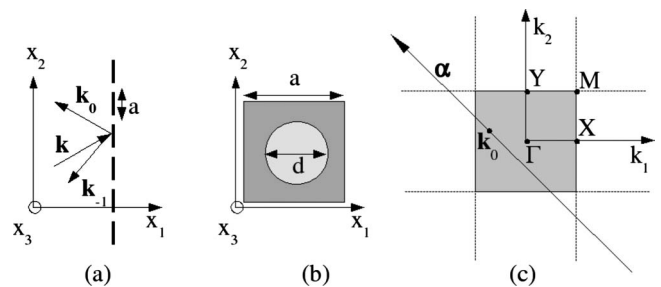


FIG. 1. (a) One-dimensional diffraction grating with pitch  $a$ . In the case depicted, the only propagative diffraction orders are those with wave vectors  $\mathbf{k}_0$  and  $\mathbf{k}_{-1}$ ; all other diffraction orders are evanescent. (b) One period of a two-dimensional square-lattice phononic crystal composed of steel rods in an epoxy matrix. (c) Representation of the reciprocal wave-vector space with the first Brillouin zone shown in gray. An arbitrary direction given by point  $\alpha$  and unit vector  $\alpha$  is shown.

The traditional way of obtaining band structures is to consider any Bloch wave vector within the first Brillouin zone and to solve for the frequency of allowed modes as  $\omega(k)$ . To obtain complex band structures, in contrast, one must consider a fixed frequency and solve for the wave vector as  $k(\omega)$ . We have specifically chosen to extend the PWE method so that it includes complex wave vectors in the direction of propagation. Notations for the PWE method are based on Ref. 17. We are looking for waves that propagate in the phononic crystal in a given arbitrary direction. From the Bloch-Floquet theorem, all fields are expressed as products of a periodic function times an exponential term  $\exp(-i\mathbf{k}\cdot\mathbf{r})$ , where  $\mathbf{k}$  is the Bloch wave vector. For instance for the three displacements ( $i=1,2,3$ )

$$u_i(\mathbf{r}) = \sum_n u_{in} \exp(-i\mathbf{G}^n\mathbf{r})\exp(-i\mathbf{k}\cdot\mathbf{r}), \quad (3)$$

where the  $\mathbf{G}^n$  are the reciprocal-lattice vectors. Note that this is a generalization of Eq. (1) to multiple periodicities. The PWE method is based on a literal application of the above formula with the summation limited to a finite number of harmonics. It can be understood as a Galerkin method with exponential functions used as the approximating functions. The basic linear PWE relations are obtained by inserting Eq. (3) in the equations of motion and read<sup>17,18</sup>

$$(iT_i) = A_{ij}\Gamma_j U, \quad (4)$$

$$\omega^2 R U = \Gamma_i (iT_i), \quad (5)$$

where summation over repeated indices is implicit ( $i,j=1,2,3$ ). The vectors  $U$  and  $T_i$  gather the Fourier amplitudes of the generalized displacements and stresses, respectively. The square matrices  $A_{ij}$  and  $R$  involve only material constants. The Bloch wave vector explicitly enters the diagonal matrices  $\Gamma_i$  defined by

$$(\Gamma_i)_{mn} = (k_i + G_i^m)\delta_{mn}. \quad (6)$$

We write  $\mathbf{k}=\mathbf{k}_0+k\boldsymbol{\alpha}$ , where  $\mathbf{k}_0$  is a constant and  $\boldsymbol{\alpha}$  is a unit vector. Some simple algebra leads from Eqs. (4) and (5) to a generalized eigenvalue problem for  $k$

$$\begin{pmatrix} -C_2 & I_d \\ \omega^2 R - B & 0 \end{pmatrix} \begin{pmatrix} U \\ iT' \end{pmatrix} = k \begin{pmatrix} D & 0 \\ C_1 & I_d \end{pmatrix} \begin{pmatrix} U \\ iT' \end{pmatrix} \quad (7)$$

with the stresses in the propagation direction  $T' = \alpha_i T_i$ ,  $B = G_i A_{ij} G_j$ ,  $C_1 = G_i A_{ij} \alpha_j$ ,  $C_2 = \alpha_i A_{ij} G_j$ ,  $D = \alpha_i A_{ij} \alpha_j$ , and  $(G_i)_{mn} = (k_{0i} + G_i^m)\delta_{mn}$ . The previous equation yields a direct solution to the  $k(\omega)$  problem, with the eigenvalue  $k$  possibly complex.

At this point, we can discuss briefly some properties of complex Bloch waves. In contrast to the traditional  $\omega(k)$  problem which assumes that  $k$  is real,<sup>12</sup>  $k(\omega)$  is not restricted from the start to the first Brillouin zone. Moreover, periodicity has not been especially enforced in the equations; it is only operating through the Bloch-Floquet decomposition of Eq. (3). We observe that only the real part of the wave vector is restricted to the first Brillouin zone while the imaginary part is unbounded. Complex Bloch waves then come as families identified by the value of their imaginary part; an arbitrary index shift in the Fourier series leads to the same

TABLE I. Independent material constants for steel and epoxy.

Material	$c_{11}$ (GPa)	$c_{44}$ (GPa)	$\rho$ (kg/m <sup>3</sup> )
Steel	287	82	7630
Epoxy	6.875	1.331	1100

solution with the real part of the wave vector shifted by an elementary lattice wave vector.

As an illustration of the properties of complex Bloch waves, we consider in this paper a two-dimensional square-lattice phononic crystal made of steel rods in epoxy, as depicted in Fig. 1(b). Despite its simplicity, this structure displays basic properties common to all phononic crystals and the analysis in this paper applies equally to materials with arbitrary anisotropy and to three-dimensional phononic crystals. The rod diameter,  $d$ , equals  $0.6 a$ , where  $a$  is the pitch of the hole array. Independent material constants used for isotropic steel and epoxy are given in Table I. Since the rod axis is aligned with the  $x_3$  axis, there is a complete decoupling of waves polarized in plane (with displacements  $u_1$  and  $u_2$  only) from pure shear waves (with displacement  $u_3$  only). This property is exploited in the representation of complex band structures shown in Fig. 2 for propagation in the  $\Gamma X$  direction. These complex band structures are divided in two adjacent panels. The right panel shows the real part of the wave vector  $k(\omega)$  while the left panel shows its imaginary part. Real parts are restricted to the first Brillouin zone but the imaginary parts are arbitrarily displayed up to  $|k|a/(2\pi)=3$  only (larger values exist).

All computations have been performed with a total of  $11 \times 11$  harmonics and the size of the matrices appearing in Eq. (6) is thus  $726 \times 726$ , owing to the six degrees of freedom (three displacements and three stresses). Complex bands have been obtained by solving the eigenvalue equation for a discrete number of frequencies and then sorted by continuity of  $k$  and polarization to obtain the displayed continuous lines. In addition, the  $\omega(k)$  problem with real  $k$ , for instance described in Refs. 17 and 19, has been solved for comparison. The traditional  $\omega(k)$  and the new  $k(\omega)$  calculation give exactly the same result for real  $k$  (for the same number of Fourier harmonics).

The most striking feature of complex bands is that there are many bands that are simply not revealed by the traditional  $\omega(k)$  method. Significantly, the occurrence of a band gap is not indicated by an absence of bands but by the evanescent character of Bloch waves. A complete band gap is traditionally defined by the condition that no propagating (real  $k$ ) solutions exist. Alternatively, we propose a definition whereby all Bloch waves must be evanescent within a complete band gap. In practice, this is a more direct and a computationally more efficient definition since it can be checked at an arbitrary frequency without plotting the full band structure.

We further observe that there is always a connection between the maximum of a real band and the minimum of another real band that is provided by a pair of complex

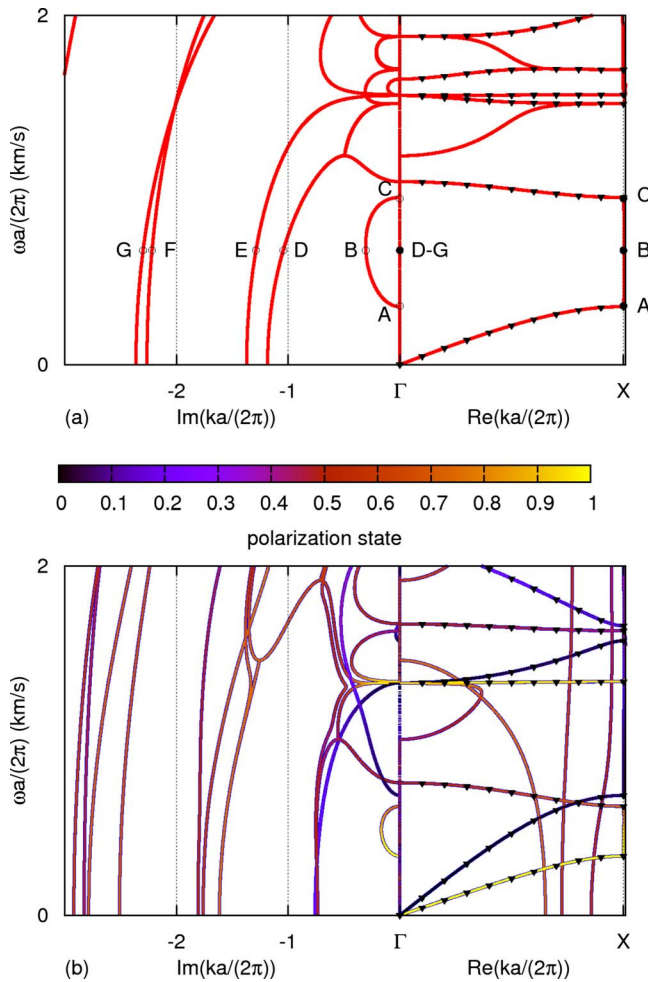


FIG. 2. (Color online) Complex band structure for a square-lattice two-dimensional phononic crystal of steel rods in epoxy in the  $\Gamma X$  direction. Band structures are (a) for pure shear Bloch waves (polarized along  $x_3$ ) and (b) for in-plane polarized Bloch waves (polarized in the  $(x_1, x_2)$  plane).  $k(\omega)$  solutions are plotted as solid lines while purely real branches obtained by the traditional  $\omega(k)$  method are represented by dots for comparison. The color scale for waves polarized in plane represents the power balance between  $u_1$  and  $u_2$  in the eigenmode (from dark for pure longitudinal to light for pure in-plane shear).

bands. This obviously happens at the symmetry points,  $\Gamma$  or  $X$ , where folding of bands is expected due to periodicity, but also inside the first Brillouin zone. Through this mechanism, the overall number of bands at any frequency is globally preserved. For instance, let us consider the evolution of the polarization of evanescent Bloch waves inside a band gap. Figure 3 displays the displacements for the points labeled A, B, and C in the complex band structure of Fig. 2(a) for the out-of-plane polarization. The three points belong to the same complex band. The modal shapes for points A (band-gap entrance) and C (band-gap exit) are concentrated inside the steel rods and inside the epoxy matrix, respectively. Inside the band gap, at point B, the situation is midway between these two extremes. Following the modal shape as the frequency varies from the entrance to the exit of the band gap, it can be observed that the energy distribution in the unit

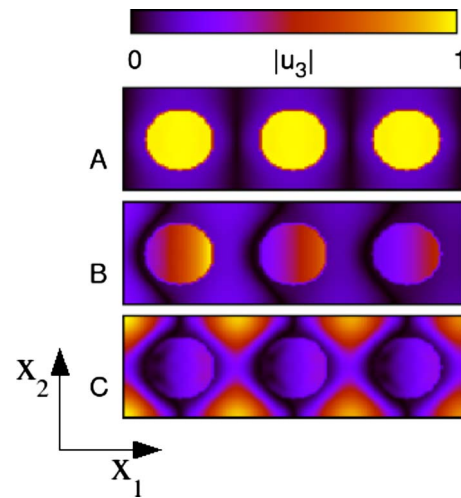


FIG. 3. (Color online) Evolution of the polarization across the lowest band gap for pure shear waves. The corresponding complex band structure is depicted in Fig. 2(a). The modulus of the displacement  $u_3$  is displayed. Points A, B, and C are for the entrance, the center, and the exit of the band gap, respectively.

cell varies continuously. We conclude that the modal shapes for evanescent Bloch waves inside a band gap are not significantly different from those for propagating Bloch waves. The modal distribution at point B further shows a moderate decay on propagation inside the phononic crystal, in accordance with the moderate value of the imaginary part of the Bloch wave vector at this point [ $Im(k) \approx -0.3 \times 2\pi/a$ ].

It can be noted that even at very low frequencies (homogenization limit), there exist evanescent waves in addition to the expected longitudinal and shear bands.<sup>20</sup> Following the evolution of such bands with increasing frequency, it can be noticed that above some cut-off frequency these initially evanescent waves become propagative. The physical origin of such evanescent Bloch waves can be understood in analogy with frustrated diffracted waves in diffraction gratings, as described by the simple model of Eqs. (1) and (2). Suppose propagation along axis  $x_1$  in Fig. 1(b), i.e., normal incidence. The wave vector  $k_2$  can be any reciprocal-lattice component  $G_2^n = 2\pi n/a$ , with  $n$  as the diffraction order. In the subdiffraction regime, i.e., for low frequencies, only the  $n=0$  order is propagative, since otherwise  $k_2/\omega$  is very large and  $k_1$  is constrained by the dispersion relation for the particular band to be complex. Now, for any value of  $n$ ,  $k_2$ , and the real part of the obtained  $k_1$  can be folded to the first Brillouin zone while the imaginary part of  $k_1$  remains unchanged. Folding of the real parts is simply accompanied by a shift in the index of  $u_{in}$  in Eq. (3). This argument can be extended to any direction of propagation and leads us to infer that in a two-dimensional phononic crystal any complex band can be associated with some diffraction order identified by a pair of indices  $(n_1, n_2)$ . In a three-dimensional phononic crystal, three indices would be necessary.

The above property is illustrated by the modal shapes depicted in Fig. 4. At the same frequency as point B, there are four evanescent Bloch bands in the complex band structure for out-of-plane waves shown in Fig. 2(a), labeled D, E, F, and G. The modal distributions at points D and E reveal that

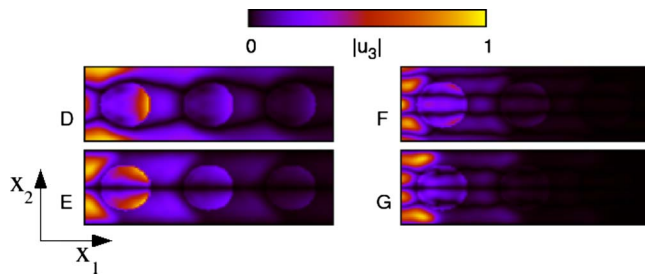


FIG. 4. (Color online) Modal distribution of evanescent Bloch waves with out-of-plane shear polarization showing oscillatory behavior along the  $x_2$  axis. The modulus of the displacement  $u_3$  is displayed for points D, E, F, and G of the complex band structure of Fig. 2(a).

there is exactly one oscillation in the transverse direction so that both evanescent Bloch waves are actually frustrated (0,1) diffraction orders. We can also observe that above some frequency, band D gets hybridized with the complex continuation of the band to which point C belongs, that is with the (0,0) diffraction order. This hybridization phenomenon between bands with different diffraction orders is actually present in all the shown complex band structures. The difference between points D and E lies in their symmetry with respect to the center of the unit cell; D (respectively, E) shows a cosine-like (respectively, sine-like) variation. The modal distributions at points F and G similarly lead us to associate them with frustrated (0,2) diffraction orders.

The concept of the complex band structure of a phononic crystal, consisting of propagating and evanescent Bloch

waves, has been introduced. Evanescent Bloch waves have been shown to arise from two closely related situations. First, within band gaps, they directly measure the exponential decrease upon transmission and they connect propagation bands, thus conserving the overall number of modes. Second, they represent higher-order diffracted waves within the crystal that are frustrated at low frequencies. This view has been supported by displaying the modal distribution of evanescent Bloch waves and observing their symmetries. Evanescent diffracted Bloch waves become propagative Bloch waves as the frequency increases thus populating the higher frequency bands. In order to obtain these results, we have extended the classical PWE method for phononic crystals so that it includes complex wave vectors in the direction of propagation. The proposed extended PWE method could well become a basic building block for solving scattering problems<sup>21</sup> in phononic crystals. Indeed, the conversion of waves at the interfaces of a finite periodic structure implies the production of evanescent waves in both the incident medium and the phononic crystal. In addition, it can model frequency-dependent material losses, through viscoelasticity (e.g., the use of complex elastic constants).<sup>22</sup> It can further directly give the equifrequency contours that are required to understand refraction (positive or negative) in phononic crystals but also the direction-dependent transmission in the band gaps.<sup>23</sup> We finally observe that the properties of evanescent Bloch waves discussed in this paper should have analogs in photonic crystals as well and more generally in any periodic medium supporting the propagation of waves.

<sup>1</sup>M. Cai, O. Painter, and K. J. Vahala, *Phys. Rev. Lett.* **85**, 74 (2000).

<sup>2</sup>F. de Fornel, *Evanescent Waves: From Newtonian Optics to Atomic Optics* (Springer, New York, 2001).

<sup>3</sup>C. Spielmann, R. Szipöcs, A. Stingl, and F. Krausz, *Phys. Rev. Lett.* **73**, 2308 (1994).

<sup>4</sup>S. Yang, J. H. Page, Z. Liu, M. L. Cowan, C. T. Chan, and P. Sheng, *Phys. Rev. Lett.* **88**, 104301 (2002).

<sup>5</sup>J. B. Pendry, *Phys. Rev. Lett.* **85**, 3966 (2000).

<sup>6</sup>R. Merlin, *Science* **317**, 927 (2007).

<sup>7</sup>A. Sentenac and P. C. Chaumet, *Phys. Rev. Lett.* **101**, 013901 (2008).

<sup>8</sup>D. M. Profunser, O. B. Wright, and O. Matsuda, *Phys. Rev. Lett.* **97**, 055502 (2006).

<sup>9</sup>R. J. P. Engelen, D. Mori, T. Baba, and L. Kuipers, *Phys. Rev. Lett.* **102**, 023902 (2009).

<sup>10</sup>E. Yablonovitch, *Phys. Rev. Lett.* **58**, 2059 (1987).

<sup>11</sup>S. John, *Phys. Rev. Lett.* **58**, 2486 (1987).

<sup>12</sup>M. S. Kushwaha, P. Halevi, L. Dobrzynski, and B. Djafari-Rouhani, *Phys. Rev. Lett.* **71**, 2022 (1993).

<sup>13</sup>F. R. Montero de Espinosa, E. Jiménez, and M. Torres, *Phys.*

*Rev. Lett.* **80**, 1208 (1998).

<sup>14</sup>A. Khelif, A. Choujaa, B. Djafari-Rouhani, M. Wilm, S. Ballandras, and V. Laude, *Phys. Rev. B* **68**, 214301 (2003).

<sup>15</sup>Y.-C. Hsue, A. J. Freeman, and B. Y. Gu, *Phys. Rev. B* **72**, 195118 (2005).

<sup>16</sup>R. Sainidou, N. Stefanou, and A. Modinos, *Phys. Rev. B* **66**, 212301 (2002).

<sup>17</sup>M. Wilm, S. Ballandras, V. Laude, and T. Pastureaud, *J. Acoust. Soc. Am.* **112**, 943 (2002).

<sup>18</sup>M. Wilm, A. Khelif, S. Ballandras, V. Laude, and B. Djafari-Rouhani, *Phys. Rev. E* **67**, 065602(R) (2003).

<sup>19</sup>V. Laude, M. Wilm, S. Benchabane, and A. Khelif, *Phys. Rev. E* **71**, 036607 (2005).

<sup>20</sup>A. A. Krokhin, J. Arriaga, and L. N. Gumen, *Phys. Rev. Lett.* **91**, 264302 (2003).

<sup>21</sup>K. Kokkonen, M. Kaivola, S. Benchabane, A. Khelif, and V. Laude, *Appl. Phys. Lett.* **91**, 083517 (2007).

<sup>22</sup>K. Ahn, Y. A. Kosevich, and M. Won Kim, *Europhys. Lett.* **60**, 241 (2002).

<sup>23</sup>F.-C. Hsu, T.-T. Wu, J.-C. Hsu, and J.-H. Sun, *Appl. Phys. Lett.* **93**, 201904 (2008).